Design of Optimal Sparse Feedback Gains via the Alternating Direction Method of Multipliers

Fu Lin, Makan Fardad, and Mihailo R. Jovanović

arXiv:1111.6188v2 [math.OC] 24 Jul 2012

Abstract

We design sparse and block sparse feedback gains that minimize the variance amplification (i.e., the $\mathcal{H}_2$ norm) of distributed systems. Our approach consists of two steps. First, we identify sparsity patterns of feedback gains by incorporating sparsity-promoting penalty functions into the optimal control problem, where the added terms penalize the number of communication links in the distributed controller. Second, we optimize state feedback gains subject to structural constraints determined by the identified sparsity patterns. This polishing step improves the quadratic performance of the distributed controller. In the first step, we identify sparsity structure of feedback gains using the alternating direction method of multipliers, which is a powerful algorithm well-suited to large optimization problems. This method alternates between promoting the sparsity of controllers and optimizing the closed-loop performance, which allows us to exploit the structure of the corresponding objective functions. In particular, we take advantage of the separability of the sparsity-promoting penalty functions to decompose the minimization problem into sub-problems that can be solved analytically. Even though the $\mathcal{H}_2$ norm is in general a nonconvex function of the feedback gain, we identify classes of convex problems that arise in the design of sparse undirected networks. We show that the corresponding synthesis problem can be formulated as a semidefinite program, implying that the globally optimal sparse controller can be computed efficiently. Several examples are provided to illustrate the effectiveness of the developed approach.

Index Terms

Alternating direction method of multipliers, communication architectures, continuation methods, convex optimization, ℓ_1 minimization, network design, semidefinite program, separable penalty functions, sparsity-promoting optimal control, structured distributed design.

I. Introduction

The design of distributed controllers for interconnected systems has received considerable attention in recent years [1]–[17]. Research efforts have focused on two major issues, namely,

Financial support from the National Science Foundation under awards CMMI-0927509 and CMMI-0927720 and under CAREER Award CMMI-0644793 is gratefully acknowledged.

F. Lin and M. R. Jovanović are with the Department of Electrical and Computer Engineering, University of Minnesota, Minneapolis, MN 55455. M. Fardad is with the Department of Electrical Engineering and Computer Science, Syracuse University, NY 13244. E-mails: fu@umn.edu, makan@syr.edu, mihailo@umn.edu.

the design of communication architectures of the distributed controllers and the design of the optimal controllers under *a priori* specified structural constraints.

The identification of convex classes of distributed control problems has been an active research topic in recent years. For spatially invariant systems, the design of quadratically optimal controllers can be cast into a convex problem if the information in the controller propagates at least as fast as in the plant [3], [6]. A similar but more general algebraic characterization of the constraint set was introduced and convexity was established under the condition of quadratic invariance in [7]. Since these convex formulations are expressed in terms of the impulse response parameters, they do not lend themselves easily to state-space characterization. In [14], a state-space realization of the optimal distributed controllers that satisfy cone-causality property was provided and methods for design of sub-optimal controllers were developed.

Characterizing the structural properties of optimal distributed controllers is another important question. For spatially invariant systems, the linear quadratic controllers are also spatially invariant and the measurements from other subsystems are exponentially discounted with the distance between the controller and the subsystems [1]. This spatially decaying property is extended to systems on graphs in [8] and it motivates the search for inherently localized controllers. Rather than truncating optimal centralized gains, an augmented Lagrangian approach was used to design structured optimal $\mathcal{H}_2$ feedback gains in [16]. Furthermore, a continuation-based Newton's method provided the optimal localized controllers for vehicular strings in [18].

In this paper, we develop methods for the design of *sparse* and *block sparse* feedback gains that minimize variance amplification of the distributed system. Our approach consists of two steps. The first step, which can be viewed as a *structure identification step*, is aimed at finding sparsity patterns $\mathcal{S}$ that strike a balance between the $\mathcal{H}_2$ performance and the sparsity of the controller. This is achieved by incorporating *sparsity-promoting* penalty functions into the optimal control problem, where the added sparsity-promoting terms penalize the number of communication links. We consider several sparsity-promoting penalty functions including the cardinality function and its convex relaxations. In the absence of sparsity-promoting terms, the solution to the standard $\mathcal{H}_2$ problem results in centralized controllers with dense feedback gains. By gradually increasing the weight on the sparsity-promoting penalty terms, the optimal feedback gain moves along a parameterized solution path from the centralized to the sparse gain of interest. This weight is increased until the desired balance between the performance and the sparsity patterns $\mathcal{S}$ is

achieved. In the second step, we solve an optimal control problem subject to the feedback gain belonging to the identified structure $\mathcal{S}$. This *polishing step* can improve the $\mathcal{H}_2$ performance of the structured controller; see [10], [16] for related efforts.

Major contributions of this paper are summarized next:

- We identify classes of convex problems that arise in several emerging applications including sparse synthesis of undirected networks of single-integrators, coordination of vehicular formations, and synchronization of oscillator networks. We show that the optimal control problem that utilizes the weighted ℓ_1 norm as the sparsity-promoting penalty function can be formulated as a semidefinite program (SDP), thereby implying that the globally optimal sparse controller can be computed efficiently.
- We demonstrate that the *alternating direction method of multipliers* (ADMM) [19] provides an effective tool for the design of sparse distributed controllers whose performance is comparable to the performance of the optimal centralized controller. This method alternates between promoting the sparsity of the feedback gain matrix and optimizing the closed-loop $\mathcal{H}_2$ norm. The advantage of this alternating mechanism is threefold. First, it provides a flexible framework for incorporation of different penalty functions that promote sparsity or block sparsity. Second, it allows us to exploit the *separability* of the sparsity-promoting penalty functions and to decompose the corresponding optimization problems into subproblems that can be solved *analytically*. These analytical results are immediately applicable to other distributed control problems where sparsity is desired. Finally, it facilitates the use of descent algorithms for the $\mathcal{H}_2$ optimization, in which a descent direction can be formed by solving two Lyapunov equations and one Sylvester equation.

Our approach is motivated in part by the emerging field of compressive sensing [20]. The ℓ_1 norm is widely used as a proxy for cardinality minimization in applied statistics, in sparse signal processing, and in machine learning; see [19], [21], [22]. In the controls community, recent work inspired by similar ideas includes [23]–[26]. In [23], an ℓ_0 induced gain was introduced to quantify the sparsity of the impulse response of a discrete-time system. In [24], [25], the weighted ℓ_1 framework was used to design structured dynamic output feedback controllers subject to a given $\mathcal{H}_\infty$ performance. In [26], an ℓ_1 relaxation method was employed for the problem of adding a fixed number of edges to a consensus network.

Our presentation is organized as follows. We formulate the sparsity-promoting optimal control

problem and compare several sparsity-promoting penalty functions in Section II. We identify classes of convex sparse synthesis problems and establish the corresponding SDP formulation in Section III. We present the ADMM algorithm, emphasize the separability of the penalty functions, and provide the analytical solutions to the sub-problems for both sparse and block sparse minimization problems in Section IV. Several examples are provided in Sections III and V to demonstrate the effectiveness of the developed approach. We conclude the paper with a summary of our contributions in Section VI.

II. Sparsity-promoting Optimal Control Problem

Consider the following control problem

$$\begin{aligned} \dot{x} &= A\,x + B_1\,d + B_2\,u \\ z &= C\,x + D\,u \\ u &= -F\,x \end{aligned} \tag{1}$$

where d and u are the disturbance and control inputs, z is the performance output, $C = \begin{bmatrix} Q^{1/2} & 0 \end{bmatrix}^T$, and $D = \begin{bmatrix} 0 & R^{1/2} \end{bmatrix}^T$, with standard assumptions that (A, B_2) is stabilizable and $(A, Q^{1/2})$ is detectable. The matrix F is a state feedback gain, $Q = Q^T \geq 0$ and $R = R^T > 0$ are the state and control performance weights, and the closed-loop system is given by

$$\begin{aligned} \dot{x} &= (A - B_2F)\,x + B_1\,d \\ z &= \begin{bmatrix} Q^{1/2} \\ -R^{1/2}F \end{bmatrix} x. \end{aligned} \tag{2}$$

The design of the optimal state feedback gain F, subject to structural constraints that dictate its zero entries, was recently considered by the authors in [10], [16]. Let the subspace $\mathcal{S}$ embody these constraints and let us assume that there exists a stabilizing $F \in \mathcal{S}$. References [10], [16] then search for $F \in \mathcal{S}$ that minimizes the $\mathcal{H}_2$ norm of the transfer function from d to z,

$$\begin{aligned} &\text{minimize} \quad J(F) \\ &\text{subject to} \quad F \in \mathcal{S} \end{aligned} \tag{SH2}$$

where

$$J(F) = \begin{cases} \operatorname{trace}\left(B_1^T P(F) B_1\right), & F \text{ stabilizing} \\ \infty, & \text{otherwise.} \end{cases} \tag{3}$$

The matrix $P(F)$ in (3) denotes the closed-loop observability Gramian

$$P(F) \;=\; \int_0^\infty \mathrm{e}^{(A-B_2F)^T t}\,(Q+F^TRF)\,\mathrm{e}^{(A-B_2F)t}\,\mathrm{d}t \tag{4}$$

which can be obtained by solving the corresponding Lyapunov equation

$$(A-B_2F)^T\,P \;+\; P\,(A-B_2F) \;=\; -\big(Q+F^TRF\big). \tag{5}$$

While the communication architecture of the controller in (SH2) is *a priori* specified, in this paper our emphasis shifts to identifying favorable communication structures without any prior assumptions on the sparsity patterns of the matrix F. We propose an optimization framework in which the sparsity of the feedback gain is directly incorporated into the objective function.

Consider the following optimization problem

$$\text{minimize}\;\; J(F) \;+\; \gamma\, g_0(F) \tag{6}$$

where

$$g_0(F) \;=\; \mathbf{card}\,(F) \tag{7}$$

denotes the cardinality function, i.e., the *number of nonzero elements* of a matrix. Note that, in contrast to problem (SH2), no structural constraint is imposed on F; instead, our goal is to promote sparsity of the feedback gain by incorporating the cardinality function into the optimization problem. The positive scalar γ characterizes our emphasis on the sparsity of F; a larger γ encourages a sparser F, while $\gamma = 0$ renders a centralized gain that is the solution of the standard LQR problem. For $\gamma = 0$, the solution to (6) is given by $F_c = R^{-1}B_2^TP$, where P is the unique positive definite solution of the algebraic Riccati equation

$$A^TP \;+\; PA \;+\; Q \;-\; PB_2R^{-1}B_2^TP \;=\; 0. \tag{8}$$

A. Sparsity-promoting penalty functions

Problem (6) is a combinatorial optimization problem whose solution usually requires an intractable combinatorial search. In optimization problems where sparsity is desired, the cardinality function is typically replaced by the ℓ_1 norm of the optimization variable [27, Chapter 6],

$$g_1(F) \;=\; \|F\|_{\ell_1} \;=\; \sum_{i,\,j} |F_{ij}|. \tag{9}$$

Recently, a *weighted* ℓ_1 norm was used to enhance sparsity in signal recovery [22],

$$g_2(F) \,=\, \sum_{i,\,j} W_{ij}|F_{ij}| \tag{10}$$

where $W_{ij} \in \mathbb{R}$ are positive weights. If W_{ij}'s are chosen to be inversely proportional to the magnitude of F_{ij}, i.e., $\{W_{ij} = 1/|F_{ij}|,\ F_{ij} \neq 0;\ W_{ij} = 1/\varepsilon,\ F_{ij} = 0,\ 0 < \varepsilon \ll 1\}$, then the weighted ℓ_1 norm and the cardinality function of F coincide, $\sum_{i,\,j} W_{ij}\,|F_{ij}| = \mathbf{card}\,(F)$.

The above scheme for the weights, however, cannot be implemented, since the weights depend on the unknown feedback gain. A reweighted algorithm that solves a sequence of weighted ℓ_1 optimization problems in which the weights are determined by the solution of the weighted ℓ_1 problem in the previous iteration was proposed in [22], [28]. This reweighted scheme was recently employed by the authors to design sparse feedback gains for a class of distributed systems [29], [30].

Both the ℓ_1 norm and its weighted version are *convex* relaxations of the cardinality function. On the other hand, we also examine utility of the *nonconvex sum-of-logs* function as a more aggressive means for promoting sparsity [22]

$$g_3(F) \,=\, \sum_{i,\,j} \log\left(1 \,+\, \frac{|F_{ij}|}{\varepsilon}\right), \quad 0 \,<\, \varepsilon \,\ll\, 1. \tag{11}$$

Remark 1: Design of feedback gains that have block sparse structure can be achieved by promoting sparsity at the level of the *submatrices* instead of at the level of the individual elements. Let the feedback gain F be partitioned into submatrices $F_{ij} \in \mathbb{R}^{m_i \times n_j}$ that need not have the same size. The weighted ℓ_1 norm and the sum-of-logs can be generalized to matrix blocks by replacing the absolute value of F_{ij} in (10) and (11) by the Frobenius norm $\|\cdot\|_F$ of F_{ij}. Similarly, the cardinality function (7) should be replaced by $\sum_{i,j} \mathbf{card}\,(\|F_{ij}\|_F)$, where $\|F_{ij}\|_F$ does not promote sparsity within the F_{ij} block; it instead promotes sparsity at the level of submatrices.

B. Sparsity-promoting optimal control problem

Our approach to sparsity-promoting feedback design makes use of the above discussed penalty functions. In order to obtain state feedback gains that strike a balance between the quadratic performance and the sparsity of the controller, we consider the following optimal control problem

$$\text{minimize} \;\; J(F) \,+\, \gamma\, g(F) \tag{SP}$$

where J is the closed-loop $\mathcal{H}_2$ norm (3) and g is a sparsity-promoting penalty function, e.g., given by (7), (9), (10), or (11). When cardinality function in (7) is replaced by (9), (10), or (11), problem (SP) can be viewed as a relaxation of the combinatorial problem (6)-(7), obtained by approximating the cardinality function with the corresponding penalty functions g.

As the parameter γ varies over $[0, +\infty)$, the solution of (SP) traces the trade-off path between the $\mathcal{H}_2$ performance J and the feedback gain sparsity g. When $\gamma = 0$, the solution is the centralized feedback gain, which can be computed from the solution of the algebraic Riccati equation (8). We then slightly increase γ and employ an iterative algorithm – the alternating direction method of multipliers (ADMM) – initialized by the optimal feedback matrix at the previous γ. The solution of (SP) becomes sparser as γ increases. After a desired level of sparsity is achieved, we fix the sparsity structure and find the optimal structured feedback gain by solving the structured $\mathcal{H}_2$ problem (SH2).

Since the set of stabilizing feedback gains is in general not convex [31] and since the matrix exponential is not necessarily a convex function of its argument [27], J need not be a convex function of F. This makes it difficult to establish convergence to the global minimum of (SP). In Section III, we identify classes of convex problems that arise in several emerging distributed control applications including sparse synthesis of undirected networks of single-integrators, coordination of vehicular formations, and synchronization of oscillator networks. Even in problems for which we cannot establish convexity of $J(F)$, our extensive computational experiments suggest that the algorithms developed in Section IV provide an effective means for attaining a desired trade-off between the $\mathcal{H}_2$ performance and the sparsity of the controller.

III. Design of Undirected Single-integrator Networks: A Convex Problem

An important question in the optimal design of networks of dynamic systems is related to the selection of interconnection topology, i.e., the identification of controller architectures that strike an optimal balance between performance and communication. The information patterns in the corresponding optimal control problem are typically described by a graph, with applications ranging from coordinated control of multi-agent systems, to average consensus in sensor networks, to synchronization of networks of oscillators [15], [18], [29], [30], [32]–[37]. Several previous research efforts have focused on characterizing performance limitations in large-scale networks with *fixed* topologies [15], [18], [33], [34], [36]–[39]. Recently, a number of authors

have considered the problem of modifying the network topology to improve its performance [26], [40]–[44].

For undirected networks of single-integrators, we next show that sparsity-promoting feedback synthesis problem (SP) with g being the weighted ℓ_1 norm can be formulated as a semidefinite program (SDP). This implies that the globally optimal sparse controller can be computed efficiently. It is worth noting that the framework of this section also bears relevance to the design of undirected networks of double-integrators that are, for example, encountered in coordination of vehicular formations and synchronization of oscillator networks.

A. A semidefinite program formulation for (SP)

For an undirected network of N single-integrators, the closed-loop system (2) is determined by

$$A = O, \quad B_1 = B_2 = I, \quad F = F^T \tag{12}$$

where I and O are $N \times N$ identity and zero matrices, and the Lyapunov equation (5) becomes

$$FP + PF = Q + FRF.$$

The closed-loop stability amounts to positive definiteness of the feedback gain, $F \succ 0$, and the objective function (3) can be expressed as

$$J(F) = (1/2)\,\mathrm{trace}\left(F^{-1}Q + RF\right). \tag{13}$$

This scenario is of interest in the design of undirected networks of single-integrator vehicles where it is desired to tightly regulate both the relative position errors between vehicles and the absolute position of the formation's center of mass [18], [29]; see Section III-B.1.

For the average consensus problem over undirected networks, however, F is a positive semidefinite Laplacian matrix of a connected graph, $F \succeq 0$, that satisfies $F\mathbb{1} = 0$ and $F + \mathbb{1}\mathbb{1}^T/N \succ 0$ with $\mathbb{1}$ denoting the vector of all ones. The state weight Q is typically selected to penalize the deviation from consensus; see Section III-B.2. If Q satisfies $Q\mathbb{1} = 0$ and $Q + \mathbb{1}\mathbb{1}^T/N \succ 0$, then the average mode $\bar{x} := (1/N)\,\mathbb{1}^T x$ associated with the eigenvector $\mathbb{1}$ of F is unobservable from the performance outputs. Consequently, the observability Gramian P satisfies $P\mathbb{1} = 0$, and it is

determined by the solution of the Lyapunov equation

$$\big(F + \mathbb{1}\mathbb{1}^T/N\big)\, P \;+\; P\,\big(F + \mathbb{1}\mathbb{1}^T/N\big) \;=\; Q \;+\; FRF$$

where the term $\mathbb{1}\mathbb{1}^T/N$ gets canceled when multiplied by P. Therefore, the objective function (3) can be expressed as

$$J(F) \;=\; (1/2)\,\mathrm{trace}\,\big((F + \mathbb{1}\mathbb{1}^T/N)^{-1}Q \;+\; RF\big). \tag{14}$$

Lemma 1: Suppose that $Q\mathbb{1} = 0$ and $Q + \mathbb{1}\mathbb{1}^T/N \succ 0$. Then the optimization problem

$$\begin{array}{lrcl} \text{minimize} & J(F) & = & (1/2)\,\mathrm{trace}\,\big((F + \mathbb{1}\mathbb{1}^T/N)^{-1}Q \;+\; R\,F\big) \\ \text{subject to} & F\,\mathbb{1} & = & 0, \quad F + \mathbb{1}\mathbb{1}^T/N \;\succ\; 0 \end{array} \tag{15}$$

can be formulated as an SDP

$$\begin{array}{ll} \underset{X,\,F}{\text{minimize}} & (1/2)\,\mathrm{trace}\,(X \;+\; R\,F) \\ \text{subject to} & \left[\begin{array}{cc} X & Q^{1/2} \\ Q^{1/2} & F + \mathbb{1}\mathbb{1}^T/N \end{array}\right] \;\succeq\; 0 \\ & F\,\mathbb{1} \;=\; 0. \end{array} \tag{16}$$

Proof: See Appendix A. ■

We now state the main result of this section.

Proposition 2: For system (2)-(12) with the objective function J given by either (13) or (14), the sparsity-promoting optimal control problem

$$\text{minimize} \;\; J(F) \;+\; \gamma \sum_{i,\,j} W_{ij}\,|F_{ij}| \tag{17}$$

can be formulated as an SDP

$$\begin{array}{ll} \underset{X,\,Y,\,F}{\text{minimize}} & (1/2)\,\mathrm{trace}\,(X \;+\; R\,F) \;+\; \gamma\,\mathbb{1}^T Y \mathbb{1} \\ \text{subject to} & \left[\begin{array}{cc} X & Q^{1/2} \\ Q^{1/2} & F + \alpha\mathbb{1}\mathbb{1}^T/N \end{array}\right] \;\succeq\; 0 \\ & \alpha\,F\,\mathbb{1} \;=\; 0 \\ & -Y \;\le\; W \circ F \;\le\; Y, \end{array} \tag{18}$$

where $\alpha = 0$ and $\alpha = 1$ correspond to J in (13) and (14), respectively.

Proof: We begin by transforming the nonsmooth weighted ℓ_1 norm in (17) to a linear function with linear inequality constraints

$$\begin{array}{ll} \underset{Y,\,F}{\text{minimize}} & J(F) \,+\, \gamma\, \mathbb{1}^T Y \mathbb{1} \\ \text{subject to} & -Y \leq W \circ F \leq Y \end{array}$$

where Y is a matrix with nonnegative elements, $Y \geq 0$, and $\circ$ is the elementwise multiplication of matrices. Using Schur complement, the minimization of J in (13) can be cast as an SDP

$$\begin{array}{ll} \underset{X,\,F}{\text{minimize}} & (1/2)\,\text{trace}\,(X \,+\, R\,F) \\ \text{subject to} & \left[\begin{array}{cc} X & Q^{1/2} \\ Q^{1/2} & F \end{array}\right] \succeq 0. \end{array} \tag{19}$$

Note that $F \succ 0$ whenever $Q \succ 0$ in the LMI in (19). This shows the equivalence between the SDP (18) with $\alpha = 0$ and the minimization problem (17) with J given by (13). Lemma 1, in conjunction with the transformation of the weighted ℓ_1 norm to linear inequality constraints, can then be used to show that the SDP (18) with $\alpha = 1$ is equivalent to the minimization problem (17) with J given by (14). This completes the proof. ■

For small and medium problems (e.g., $N \leq 50$), the global solution of (17) can be obtained using standard SDP solvers. For large problems, customized interior point method can be developed to solve (17); see [42] for related problems. Alternatively, the ADMM algorithm developed in Section IV provides a powerful tool for large-scale optimal control problems given by (SP).

Remark 2: The above presented framework for the design of undirected networks of single-integrators is also relevant for the design of undirected networks with higher order sub-systems [18], [30]. For an undirected network of double-integrator vehicles with uniform diagonal velocity gain, the design of a symmetric position gain matrix to maintain a desired spacing between the vehicles amounts to minimization of J given by (13); see [18]. For a network of LC-oscillators with identical oscillation frequency, the design of the conductance matrix to keep small difference in voltage among oscillators amounts to minimization of J given by (14); see [30]. Thus, these design problems can be also addressed using the SDP-formulation presented in Proposition 2.

B. Examples

To illustrate utility of Proposition 2, we next provide examples that are encountered in the design of sparse vehicular formation and average consensus networks. We show that these classes of problems can be formulated as the SDP (18).

1) Leader-follower vehicular formation: Consider N single-integrator vehicles

$$\dot{x}_i \,=\, u_i \,+\, d_i, \qquad i = 1, \ldots, N$$

where u_i and d_i are the control and the disturbance acting on the ith vehicle. A vehicle is a follower if it uses only the relative information exchange with other vehicles to compute its control action,

$$u_i \,=\, -\sum_{j\,=\,1,\,j\,\neq\,i}^{N} F_{ij}\,(x_i - x_j).$$

A vehicle is a leader if, in addition to the relative information exchange with other vehicles, it also has access to its own state

$$u_i \,=\, -\sum_{j\,=\,1,\,j\,\neq\,i}^{N} F_{ij}\,(x_i - x_j) \,-\, F_{ii}\,x_i.$$

For a formation shown in Fig. 1, with the 1st and the Nth vehicles being leaders and all other vehicles being followers, we penalize both the absolute position errors of the vehicles

$$x^T Q_g\, x \,=\, \sum_{i\,=\,1}^{N} x_i^2$$

and the relative position errors between the vehicles

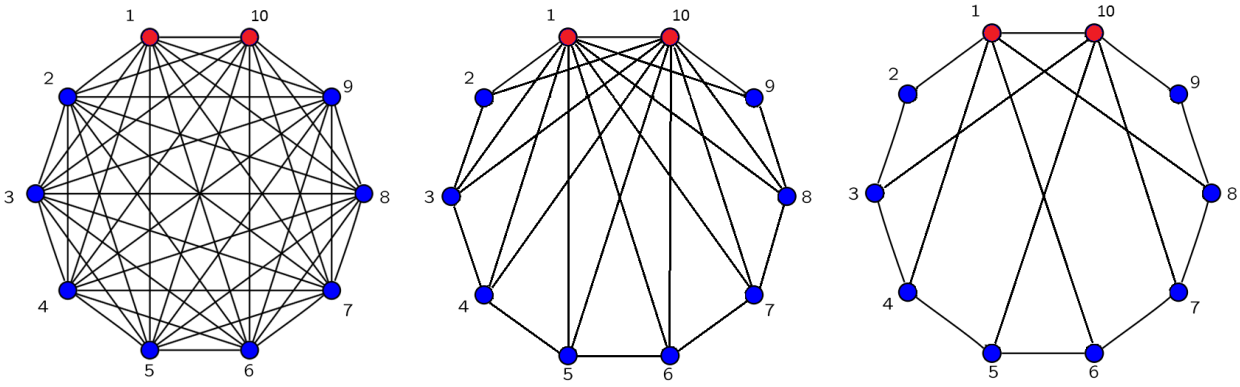
$$x^T Q_l\, x \,=\, \sum_{i\,=\,1}^{N-1} \left(x_i \,-\, x_{i+1}\right)^2.$$

Thus, $Q_g = I$ and Q_l is a symmetric tridiagonal matrix with -1 on its first sub- and super-diagonal; the first and the last elements on the main diagonal of Q_l are equal to 1, and all other elements on its main diagonal are equal to 2. We set $Q = Q_g + Q_l$ and choose $R = I$.

The communication graphs determined by sparsity structures of F for different values of γ are illustrated in Fig. 2. For $\gamma = 0$, we have a centralized controller in which all-to-all communication is required in order to form the control action; for $\gamma = 0.02$, a star-like topology with respect to



Fig. 1: One-dimensional vehicular formation with the 1st and the Nth vehicles being leaders (highlighted in red color) and all other vehicles being followers.



(a) $\gamma = 0$ (b) $\gamma = 0.02$ (c) $\gamma = 0.06$

Fig. 2: For illustration purpose, we wrap the communication graph of the formation around a circle. (a) All-to-all communication architecture for $\gamma = 0$; (b) leaders-to-all plus nearest neighbor interaction for $\gamma = 0.02$; (c) leaders-to-some plus nearest neighbor interaction for $\gamma = 0.06$.

leaders is identified; and for $\gamma = 0.06$, we obtain a controller with leaders-to-some plus nearest neighbor interactions. We note that the number of vehicles that communicate with the leaders decreases with γ, and that the nearest neighbor interaction pattern emerges for large values of γ.

2) Undirected consensus networks: Consider an undirected connected network with N nodes in which each node updates its scalar state using a weighted average of differences between its own state and the states of its neighbors

$$\dot{x}_i = -\sum_{j \in \mathcal{N}_i} F_{ij} (x_i - x_j) + d_i.$$

This problem can be viewed as either the vehicular formation problem without leaders or as a sensor network problem in which the sensors are trying to reach consensus. Since the leaderless network with only relative information exchange is not asymptotically stable, the average of all states $\bar{x} := (1/N)\, \mathbb{1}^T x$ in the presence of stochastic disturbances undergoes a random walk [33].

Following [36], we consider the local and global performance errors that render the average mode $\bar{x}$ unobservable. The global error quantifies the deviation of each node's state from the average of all states

$$(z_g)_i \;=\; x_i \;-\; \bar{x} \;=\; x_i \;-\; \frac{1}{N}\sum_{i=1}^{N} x_i.$$

In contrast, the local error quantifies the difference between the states of neighboring nodes

$$(z_l)_{ij} \;=\; x_i \;-\; x_j \;\text{ for }\; (i,j) \;\in\; \mathcal{E}$$

where $\mathcal{E}$ is the edge set with $(i,j) \in \mathcal{E}$ denoting an edge between two neighboring nodes.

For $N = 50$ randomly distributed nodes in a region of 10×10 units, let two nodes be neighbors if their Euclidean distance is not greater than 2 units; see Fig. 3a. Thus, the performance output is given by

$$z \;=\; \left[\begin{array}{ccc} z_l^T & z_g^T & u^T \end{array}\right]^T \;=\; \left[\begin{array}{ccc} \left(Q_l^{1/2}\, x\right)^T & \left((I \,-\, \mathbb{1}\mathbb{1}^T/N)\, x\right)^T & u^T \end{array}\right]^T$$

where $Q_l = E\,E^T$ and E is the incidence matrix of the local performance graph.

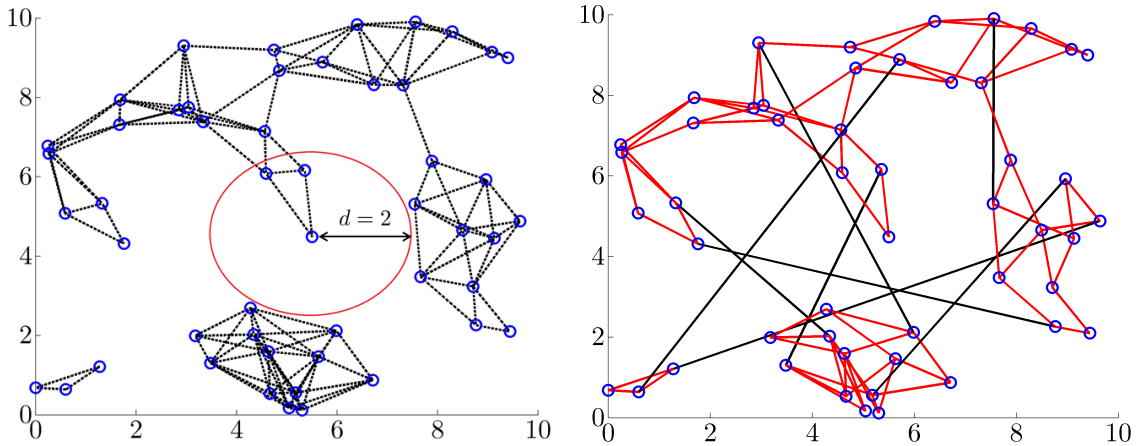
As shown in Fig. 3b, in addition to the interactions between neighbors, the identified communication graph also establishes long-range links between selected pairs of remote nodes. Relative to the centralized gain F_c, the identified sparse gain F uses 7% nonzero elements (i.e., $\mathbf{card}(F)/\mathbf{card}(F_c) = 7\%$) and achieves a performance loss of only 14% (i.e., $(J - J_c)/J_c = 14\%$). The optimal gains are obtained by solving the SDP (18) with $\alpha = 1$, $\gamma = 0$ (for F_c), and $\gamma = 1$ (for F).

IV. Identification of Sparsity-patterns via ADMM

The alternating direction method of multipliers (ADMM) has been studied extensively since the 1970s. This simple but powerful algorithm blends the separability of the dual decomposition with the superior convergence and robustness of the method of multipliers [19]. As a consequence, it has been employed in a wide range of applications [45]–[47]; reference [19] provides an excellent survey with emphasis on its application to large-scale distributed optimization problems.

Consider the following constrained optimization problem

$$\begin{array}{ll} \text{minimize} & J(F) \,+\, \gamma\, g(G) \\ \text{subject to} & F \,-\, G \,=\, 0 \end{array} \tag{20}$$



(a) (b) $\gamma = 1$

Fig. 3: (a) Local performance graph where edges connect every pair of nodes with a distance not greater than 2 units. (b) Identified communication graph for $\gamma = 1$, where the long-range communication links are highlighted in black color.

which is clearly equivalent to the problem (SP). The augmented Lagrangian associated with the constrained problem (20) is given by

$$\mathcal{L}_\rho(F, G, \Lambda) \;=\; J(F) \,+\, \gamma\, g(G) \,+\, \mathrm{trace}\left(\Lambda^T(F \,-\, G)\right) \,+\, \frac{\rho}{2}\|F \,-\, G\|_F^2$$

where Λ is the dual variable (i.e., the *Lagrange multiplier*), ρ is a positive scalar, and $\|\cdot\|_F$ is the Frobenius norm. By introducing an additional variable G and an additional constraint $F - G = 0$, we have simplified the problem (SP) by decoupling the objective function into two parts that depend on two different variables. As discussed below, this allows us to exploit the structures of J and g. We note that reference [19] provides many examples of such equivalent problem formulations suitable for the application of ADMM.

In order to find a minimizer of the constrained problem (20), the ADMM algorithm uses a sequence of iterations

$$F^{k+1} \;:=\; \arg\min_F \; \mathcal{L}_\rho(F, G^k, \Lambda^k) \tag{21a}$$

$$G^{k+1} \;:=\; \arg\min_G \; \mathcal{L}_\rho(F^{k+1}, G, \Lambda^k) \tag{21b}$$

$$\Lambda^{k+1} \;:=\; \Lambda^k \,+\, \rho(F^{k+1} \,-\, G^{k+1}) \tag{21c}$$

until $\|F^{k+1} - G^{k+1}\|_F \leq \epsilon$ and $\|G^{k+1} - G^k\|_F \leq \epsilon$. In contrast to the *method of multipliers* [19],

in which F and G are *minimized jointly*,

$$(F^{k+1}, G^{k+1}) := \underset{F,\,G}{\arg\min}\ \mathcal{L}_\rho(F, G, \Lambda^k)$$

ADMM consists of an F-minimization step (21a), a G-minimization step (21b), and a dual variable update step (21c). Thus, the optimal F and G are determined in an alternating fashion, which motivates the name *alternating direction*. Note that the dual variable update (21c) uses a step-size equal to ρ, which guarantees that one of the dual feasibility conditions is satisfied in each ADMM iteration; see [19, Section 3.3].

ADMM brings two major benefits to the sparsity-promoting optimal control problem (SP):

- *Separability of g.* The penalty function g is *separable* with respect to the *individual* elements of the matrix. In contrast, the closed-loop $\mathcal{H}_2$ norm cannot be decomposed into componentwise functions of the feedback gain. By separating g and J in the minimization of the augmented Lagrangian $\mathcal{L}_\rho$, we can decompose G-minimization problem (21b) into sub-problems that only involve *scalar* variables. This allows us to determine *analytically* the solution of (21b).
- *Differentiability of J.* The closed-loop $\mathcal{H}_2$ norm J is a *differentiable* function of the feedback gain matrix [16]; this is in sharp contrast to g which is a *non-differentiable* function. By separating g and J in the minimization of the augmented Lagrangian $\mathcal{L}_\rho$, we can utilize descent algorithms that rely on the differentiability of J to solve the F-minimization problem (21a).

We next provide the analytical expressions for the solutions of the G-minimization problem (21b) in Section IV-A, describe a descent method to solve the F-minimization problem (21a) in Section IV-B, present Newton's method to solve the structured problem (SH2) in Section IV-C, and discuss the convergence of ADMM in Section IV-D.

A. *Separable solution to the G-minimization problem* (21b)

The completion of squares with respect to G in the augmented Lagrangian $\mathcal{L}_\rho$ can be used to show that (21b) is equivalent to

$$\text{minimize}\quad \phi(G) \,=\, \gamma\, g(G) \,+\, (\rho/2)\|G \,-\, V^k\|_F^2 \tag{22}$$

where $V^k = (1/\rho)\Lambda^k + F^{k+1}$. To simplify notation, we drop the superscript k in V^k throughout this section. Since both g and the square of the Frobenius norm can be written as a summation

of componentwise functions of a matrix, we can decompose (22) into sub-problems expressed in terms of the *individual* elements of G. For example, if g is the weighted ℓ_1 norm, then

$$\phi(G) \;=\; \sum_{i,j} \Big(\gamma\, W_{ij}\, |G_{ij}| \;+\; (\rho/2)(G_{ij} \;-\; V_{ij})^2 \Big).$$

This facilitates the conversion of (22) to minimization problems that only involve *scalar* variables G_{ij}. By doing so, the solution of (22) for different penalty functions can be determined *analytically* including the weighted ℓ_1 norm, the sum-of-logs function, and the cardinality function.

1) Weighted ℓ_1 norm: The unique solution to (22) is given by the *soft thresholding* operator (e.g., see [19, Section 4.4.3])

$$G_{ij}^\star \;=\; \begin{cases} \left(1 \;-\; \dfrac{a}{|V_{ij}|}\right) V_{ij}, & |V_{ij}| \;>\; a \\ 0, & |V_{ij}| \;\leq\; a \end{cases} \tag{23}$$

where $a = (\gamma/\rho)W_{ij}$; see Fig. 4a for an illustration. For given V_{ij}, $G_{ij}^\star$ is obtained by moving V_{ij} towards zero with the amount $(\gamma/\rho)W_{ij}$. In particular, $G_{ij}^\star$ is set to zero if $|V_{ij}| \leq (\gamma/\rho)W_{ij}$, implying that a more aggressive scheme for driving $G_{ij}^\star$ to zero can be obtained by increasing γ and W_{ij} and by decreasing ρ.

2) Cardinality function: The unique solution to (22) is given by the *truncation* operator

$$G_{ij}^\star \;=\; \begin{cases} V_{ij}, & |V_{ij}| \;>\; b \\ 0, & |V_{ij}| \;\leq\; b \end{cases} \tag{24}$$

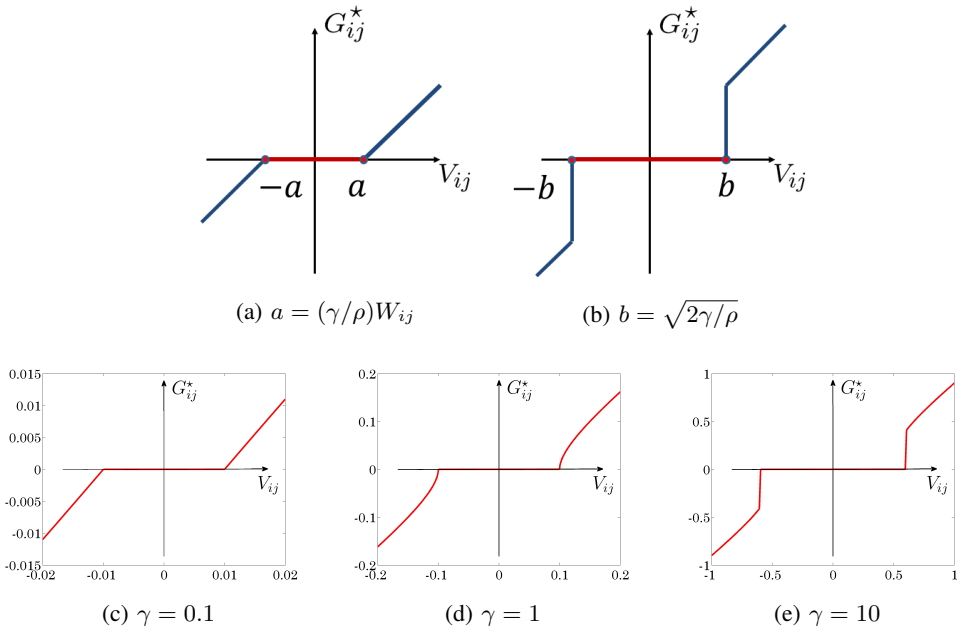
where $b = \sqrt{2\gamma/\rho}$; see Fig. 4b for an illustration. For given V_{ij}, $G_{ij}^\star$ is set to V_{ij} if $|V_{ij}| > \sqrt{2\gamma/\rho}$ and to zero if $|V_{ij}| \leq \sqrt{2\gamma/\rho}$.

3) Sum-of-logs function: As shown in Appendix C, the solution to (22) is given by

$$G_{ij}^\star \;=\; \begin{cases} 0, & \Delta \;\leq\; 0 \\ 0, & \Delta \;>\; 0 \text{ and } r^+ \;\leq\; 0 \\ r^+, & \Delta \;>\; 0 \text{ and } r^- \;\leq\; 0 \text{ and } 0 \;<\; r^+ \;\leq\; 1 \\ G^0, & \Delta \;>\; 0 \text{ and } 0 \;\leq\; r^\pm \;\leq\; 1 \end{cases} \tag{25}$$

where

$$\begin{aligned} \Delta \;&=\; (|V_{ij}| + \varepsilon)^2 - 4(\gamma/\rho) \\ r^\pm \;&=\; \frac{1}{2|V_{ij}|} \Big(|V_{ij}| \;-\; \varepsilon \;\pm\; \sqrt{\Delta} \Big) \end{aligned} \tag{26}$$



(a) $a = (\gamma/\rho)W_{ij}$ (b) $b = \sqrt{2\gamma/\rho}$

(c) $\gamma = 0.1$ (d) $\gamma = 1$ (e) $\gamma = 10$

Fig. 4: (a) The soft thresholding operator (23); (b) the truncation operator (24). The slope of the lines in both (a) and (b) is equal to one. (c)-(e) The operator (25) with $\{\rho = 100,\ \varepsilon = 0.1\}$ for different values of γ. For $\gamma = 0.1$, (25) resembles the soft thresholding operator (23) in Fig. 4a; for $\gamma = 10$, it resembles the truncation operator (24) in Fig. 4b; for $\gamma = 1$, operator (25) bridges the difference between the soft thresholding and truncation operators.

and $G^0 := \arg\min\{\phi_{ij}(r^+V_{ij}), \phi_{ij}(0)\}$. For fixed ρ and ε, (25) is determined by the value of γ; see Figs. 4c-4e. For small γ, (25) resembles the soft thresholding operator (cf. Figs. 4c and 4a) and for large γ, it resembles the truncation operator (cf. Figs. 4e and 4b). In other words, (25) can be viewed as an intermediate step between the soft thresholding and the truncation operators.

Remark 3: In block sparse design, g is determined by $\left\{\sum_{i,j} W_{ij}\|G_{ij}\|_F;\ \sum_{i,j} \mathbf{card}\,(\|G_{ij}\|_F);\ \sum_{i,j} \log(1 + \|G_{ij}\|_F/\varepsilon)\right\}$, and the minimizers of (22) are obtained by replacing the absolute value of V_{ij} in (23), (24), and (26), respectively, with the Frobenius norm $\|\cdot\|_F$ of the corresponding block submatrix V_{ij}.

B. Anderson-Moore method for the F-minimization problem (21a)

We next employ the Anderson-Moore method to solve the F-minimization problem (21a). The advantage of this algorithm lies in its fast convergence (compared to the gradient method) and in its simple implementation (compared to Newton's method); e.g., see [16], [48], [49]. When applied to the F-minimization problem (21a), this method requires the solutions of two

Lyapunov equations and one Sylvester equation in each iteration. We next recall the first and second order derivatives of J; for related developments, see [49].

Proposition 3: The gradient of J is determined by

$$\nabla J(F) \;=\; 2\,(RF - B_2^T P)\,L$$

where L and P are the controllability and observability Gramians of the closed-loop system,

$$(A \,-\, B_2F)\,L \,+\, L\,(A \,-\, B_2F)^T \;=\; -\,B_1B_1^T \tag{NC-L}$$

$$(A \,-\, B_2F)^T\,P \,+\, P\,(A \,-\, B_2F) \;=\; -\,(Q \,+\, F^TRF). \tag{NC-P}$$

The second-order approximation of J is determined by

$$J(F+\tilde{F}) \;\approx\; J(F) \,+\, \langle \nabla J(F), \tilde{F}\rangle \,+\, (1/2)\,\langle H(F,\tilde{F}),\tilde{F}\rangle$$

where $H(F,\tilde{F})$ is the linear function of $\tilde{F}$,

$$H(F,\tilde{F}) \;=\; 2\left((R\tilde{F} - B_2^T\tilde{P})\,L \,+\, (RF - B_2^TP)\,\tilde{L}\right)$$

and $\tilde{L}$, $\tilde{P}$ are the solutions of the following Lyapunov equations

$$\begin{aligned}
&(A - B_2F)\,\tilde{L} \,+\, \tilde{L}\,(A - B_2F)^T \;=\; B_2\tilde{F}L \,+\, (B_2\tilde{F}L)^T\\
&(A - B_2F)^T\,\tilde{P} \,+\, \tilde{P}\,(A - B_2F) \;=\; (PB_2 - F^TR)\,\tilde{F} \,+\, \tilde{F}^T\,(B_2^TP - RF).
\end{aligned}$$

By completing the squares with respect to F in the augmented Lagrangian $\mathcal{L}_\rho$, we obtain the following equivalent problem to (21a)

$$\text{minimize}\;\; \varphi(F) \;=\; J(F) \,+\, (\rho/2)\|F \,-\, U^k\|_F^2$$

where $U^k \;=\; G^k \,-\, (1/\rho)\Lambda^k$. Setting $\nabla\varphi \;:=\; \nabla J + \rho(F - U^k)$ to zero yields the necessary conditions for optimality

$$2\left(RF \,-\, B_2^TP\right)L \,+\, \rho\left(F \,-\, U^k\right) \;=\; 0 \tag{NC-F}$$

where L and P are determined by (NC-L) and (NC-P).

Starting with a stabilizing feedback F, the Anderson-Moore method solves the two Lyapunov equations (NC-L) and (NC-P), and then solves the Sylvester equation (NC-F) to obtain a new feedback gain $\bar{F}$. In other words, it alternates between solving (NC-L) and (NC-P) for L and P

with F being fixed and solving (NC-F) for F with L and P being fixed. It can be shown that the difference between two consecutive steps $\tilde{F} = \bar{F} - F$ forms a descent direction of φ; see [16] for a related result. Thus, standard line search [50] can be employed to determine step-size s in $F + s\tilde{F}$ to guarantee the convergence to a stationary point of φ.

Remark 4 (Closed-loop stability): Since the $\mathcal{H}_2$ norm is well defined for causal, strictly proper, stable closed-loop systems, we set J to infinity if $A - B_2F$ is not Hurwitz. Furthermore, J is a smooth function that increases to infinity as one approaches the boundary of the set of stabilizing gains [16]. Thus, the decreasing sequence of $\{\varphi(F^i)\}$ ensures that $\{F^i\}$ are stabilizing gains.

Remark 5: For the design of single-integrator networks (17), we use Newton's method to solve the F-minimization problem and provide the gradient and Hessian of J in Appendix B.

C. Solving the structured $\mathcal{H}_2$ problem: Polishing step

We next turn to the $\mathcal{H}_2$ problem subject to structural constraints on the feedback matrix. Here, we fix the sparsity patterns $F \in \mathcal{S}$ identified using ADMM and then solve (SH2) to obtain the optimal feedback gain that belongs to the subspace $\mathcal{S}$. This *polishing* step, which is commonly used in optimization [27, Section 6.3.2], can improve the performance of sparse feedback gains resulting from the ADMM algorithm.

As noted in Remark 4, the sparse feedback gains obtained in the ADMM algorithm are stabilizing. This feature of ADMM facilitates the use of Newton's method to solve (SH2). Given an initial gain $F^0 \in \mathcal{S}$, a decreasing sequence of the objective function $\{J(F^i)\}$ is generated by updating F according to $F^{i+1} = F^i + s^i\,\tilde{F}^i$; here, s^i is the step-size and $\tilde{F}^i \in \mathcal{S}$ is the Newton direction that is determined by the minimizer of the second-order approximation of the objective function (3). Equivalently, $\tilde{F}^i \in \mathcal{S}$ is the minimizer of

$$\Phi(\tilde{F}) \;:=\; (1/2)\,\langle H(\tilde{F}) \circ I_{\mathcal{S}}, \tilde{F}\rangle \;+\; \langle \nabla J \circ I_{\mathcal{S}}, \tilde{F}\rangle$$

where *structural identity* $I_{\mathcal{S}}$ of subspace $\mathcal{S}$ (under entry-wise multiplication $\circ$ of two matrices) is used to characterize structural constraints

$$I_{\mathcal{S}ij} \;=\; \begin{cases} 1, & \text{if } F_{ij} \text{ is a free variable} \\ 0, & \text{if } F_{ij} = 0 \text{ is required} \end{cases} \qquad \Rightarrow \quad F \circ I_{\mathcal{S}} \;=\; F \;\; \text{for} \;\; F \in \mathcal{S}.$$

To compute Newton direction, we use the conjugate gradient (CG) method that does not require forming or inverting the large Hessian matrix explicitly; see [50, Chapter 5]. It is noteworthy that

techniques such as the negative curvature test [50, Section 7.1] can be employed to guarantee the descent property of Newton direction; consequently, line search methods, such as Armijo rule [50, Section 3.1], can be used to generate a decreasing sequence of J.

D. Convergence of ADMM

For convex problems, e.g., the design of single-integrator networks with the weighted ℓ_1 norm as the sparsity-promoting penalty function, the convergence of ADMM to the global minimizer follows from standard results [19]. For nonconvex problems, where convergence results are not available, extensive computational experience suggests that ADMM works well when the value of ρ is sufficiently large [51], [52]. This is attributed to the quadratic term $(\rho/2)\|F-G\|_F^2$ that tends to locally convexify the objective function for sufficiently large ρ; see [53, Chapter 14.5].

We next examine convergence of the ADMM algorithm for problem (SP) with g determined by the weighted ℓ_1 norm (10). In this case, we show that when ADMM converges it converges to a critical point of (SP). For a convergent point $(F^\star, G^\star, \Lambda^\star)$ of the sequence $\{F^k, G^k, \Lambda^k\}$, (21c) simplifies to

$$F^\star \,-\, G^\star \,=\, 0.$$

Since $F^\star$ minimizes $\mathcal{L}_\rho(F, G^\star, \Lambda^\star)$ and since $G^\star$ minimizes $\mathcal{L}_\rho(F^\star, G, \Lambda^\star)$, we have

$$\begin{aligned} 0 \;&=\; \nabla J(F^\star) \,+\, \Lambda^\star \\ 0 \;&\in\; \gamma\, \partial g(G^\star) \,-\, \Lambda^\star \end{aligned}$$

where ∂g is the subdifferential of the convex function g in (10). Therefore, $(F^\star, G^\star)$ satisfies the necessary conditions for the optimality of (SP) and ADMM converges to a critical point of (SP).

V. Examples

We next use three examples to illustrate the utility of the approach developed in Section IV. The identified sparsity structures result in *localized* controllers in all three cases. Additional information about these examples, along with MATLAB source codes, can be found at

www.ece.umn.edu/∼mihailo/software/lqrsp/

A. Mass-spring system

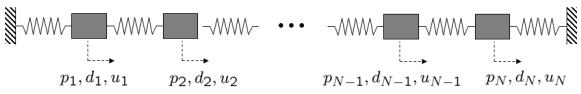


Fig. 5: Mass-spring system.

For a mass-spring system with N masses shown in Fig. 5, let p_i be the displacement of the ith mass from its reference position and let the state variables be $x_1 := [\, p_1 \cdots p_N \,]^T$ and $x_2 := [\, \dot{p}_1 \cdots \dot{p}_N \,]^T$. For simplicity we consider unit masses and spring constant; note that our method can be used to design controllers for arbitrary values of these parameters. The state-space representation is then given by (1) with

$$A \;=\; \begin{bmatrix} O & I \\ T & O \end{bmatrix}, \quad B_1 \;=\; B_2 \;=\; \begin{bmatrix} O \\ I \end{bmatrix},$$

where T is an $N \times N$ symmetric tridiagonal matrix with -2 on its main diagonal and 1 on its first sub- and super-diagonal, and I and O are $N \times N$ identity and zero matrices. The state performance weight Q is the identity matrix and the control performance weight is $R = 10I$.

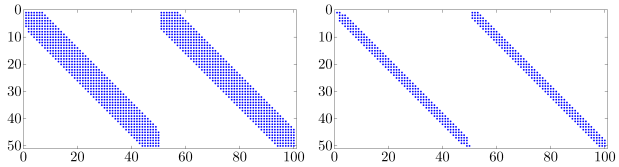
We use the weighted ℓ_1 norm as the sparsity-promoting penalty function, where we follow [22] and set the weights W_{ij} to be inversely proportional to the magnitude of the solution $F^\star$ of (SP) at the previous value of γ,

$$W_{ij} = 1/(|F^\star_{ij}| + \varepsilon). \tag{27}$$

This places larger relative weight on smaller feedback gains and they are more likely to be dropped in the sparsity-promoting algorithm. Here, $\varepsilon = 10^{-3}$ is introduced to have well-defined weights when $F^\star_{ij} = 0$.

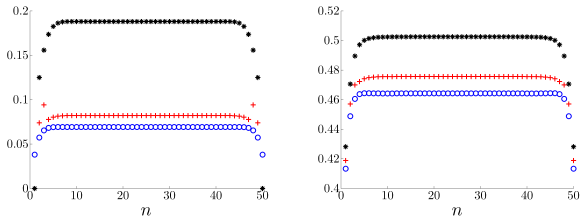
The optimal feedback gain at $\gamma = 0$ is computed from the solution of the algebraic Riccati equation (8). As γ increases, the number of nonzero sub- and super-diagonals of both position $F^\star_p$ and velocity $F^\star_v$ gains decreases; see Fig. 6. Eventually, both $F^\star_p$ and $F^\star_v$ become diagonal matrices. It is noteworthy that diagonals of both position and velocity feedback gains are nearly constant except for masses that are close to the boundary; see Fig. 7.

After sparsity structures of controllers are identified by solving (SP), we fix sparsity patterns and solve structured $\mathcal{H}_2$ problem (SH2) to obtain the optimal *structured* controllers. Comparing the sparsity level and the performance of these controllers to those of the centralized controller



(a) $\gamma = 10^{-4}$ (b) $\gamma = 0.0105$

Fig. 6: Sparsity patterns of $F^\star = [F_p^\star \quad F_v^\star] \in \mathbb{R}^{50\times 100}$ for the mass-spring system obtained using weighted ℓ_1 norm to promote sparsity. As γ increases, the number of nonzero sub- and super-diagonals of $F_p^\star$ and $F_v^\star$ decreases.



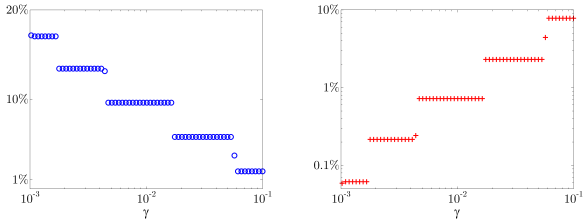
(a) (b)

Fig. 7: (a) The diagonal of $F_p^\star$ and (b) the diagonal of $F_v^\star$ for different values of γ: 10^{-4} ($\circ$), 0.0281 ($+$), and 0.1 ($*$). The diagonals of the centralized position and velocity gains are almost identical to ($\circ$) for $\gamma = 10^{-4}$.

F_c, we see that using only a *fraction* of nonzero elements, the sparse feedback gain $F^\star$ achieves $\mathcal{H}_2$ performance comparable to the performance of F_c; see Fig. 8. In particular, using about 2% of nonzero elements, $\mathcal{H}_2$ performance of $F^\star$ is only about 8% worse than that of F_c; see Table I.

γ	0.01	0.04	0.10
$\mathbf{card}\,(F^\star)/\mathbf{card}\,(F_c)$	9.4%	5.8%	2.0%
$(J(F^\star) - J(F_c))/J(F_c)$	0.8%	2.3%	7.8%

TABLE I: Sparsity vs. performance for mass-spring system. Using 2% of nonzero elements, $\mathcal{H}_2$ performance of $F^\star$ is only 7.8% worse than performance of the centralized gain F_c.



(a) $\mathbf{card}\,(F^\star)/\mathbf{card}\,(F_c)$ (b) $(J(F^\star)\,-\,J(F_c))/J(F_c)$

Fig. 8: (a) The sparsity level and (b) the performance loss of $F^\star$ compared to the centralized gain F_c.

B. Spatially distributed example

Let $N = 100$ nodes be randomly distributed with a uniform distribution in a square region of 10×10 units. Each node is a linear system coupled with other nodes through the dynamics [8]

$$\dot{x}_i \,=\, \sum_{j\,=\,1}^{N} [A]_{ij}\, x_j \,+\, [B_1]_{ii}\, d_i \,+\, [B_2]_{ii}\, u_i$$

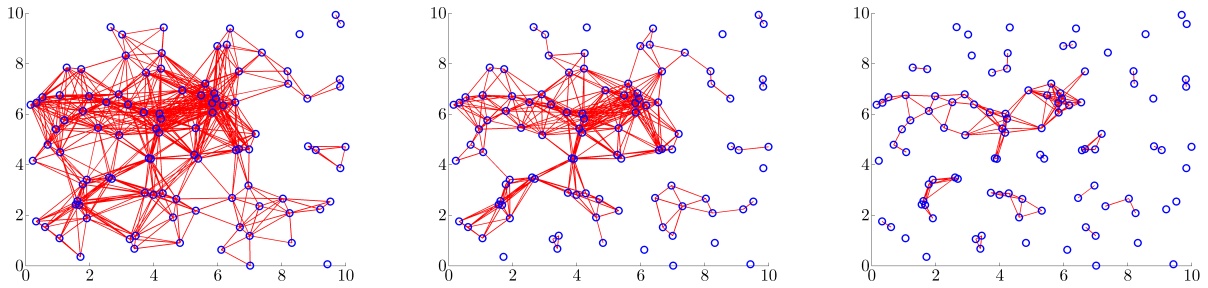
for $i = 1, \ldots, N$, where $[\,\cdot\,]_{ij}$ denotes the ijth block of a matrix and

$$[A]_{ii} \,=\, \begin{bmatrix} 1 & 1 \\ 1 & 2 \end{bmatrix}, \quad [B_1]_{ii} \,=\, [B_2]_{ii} \,=\, \begin{bmatrix} 0 \\ 1 \end{bmatrix}, \quad [A]_{ij} \,=\, \frac{1}{\mathrm{e}^{\alpha(i,j)}} \begin{bmatrix} 1 & 0 \\ 0 & 1 \end{bmatrix}, \quad \text{for} \quad i \neq j.$$

The coupling between two systems i and j is determined by the Euclidean distance $\alpha(i,j)$ between them. The performance weights Q and R are set to identity matrices.

We use the weighted ℓ_1 norm as the penalty function with the weights given by (27). As γ increases, the communication architecture of distributed controllers becomes sparser. Furthermore, the underlying communication graphs gradually attain a *localized* communication architecture; see Fig. 9. Note that, using about 8% of nonzero elements of F_c, $\mathcal{H}_2$ performance of $F^\star$ is only about 28% worse than performance of the centralized gain F_c; see Table II. Figure 10 shows the optimal trade-off curve between the $\mathcal{H}_2$ performance and the feedback gain sparsity.

We note that the truncation of the centralized controller could result in a non-stabilizing feedback matrix [8]. In contrast, our approach gradually modifies the feedback gain and increases the number of zero elements, which plays an important role in preserving the closed-loop stability.



(a) $\gamma = 12.6$ (b) $\gamma = 26.8$ (c) $\gamma = 68.7$

Fig. 9: The localized communication graphs of distributed controllers obtained by solving (SP) for different values of γ. The communication structure becomes sparser as γ increases. Note that the communication graph does not have to be connected since the subsystems are (i) dynamically coupled to each other and (ii) allowed to measure their own states.

γ	12.6	26.8	68.7
$\mathbf{card}\,(F^\star)/\mathbf{card}\,(F_c)$	8.3%	4.9%	2.4%
$(J(F^\star) - J(F_c))/J(F_c)$	27.8%	43.3%	55.6%

TABLE II: Sparsity vs. performance for the spatially distributed example. Using 8.3% of nonzero elements, $\mathcal{H}_2$ performance of $F^\star$ is only 27.8% worse than performance of the centralized gain F_c.

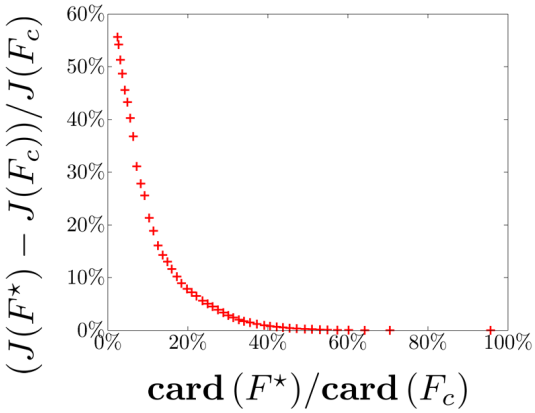


Fig. 10: The optimal trade-off curve between the $\mathcal{H}_2$ performance loss and the sparsity level of $F^\star$ compared to the centralized gain F_c for the spatially distributed example.

C. Block sparsity: An example from bio-chemical reaction

Consider a network of $N = 5$ systems coupled through the following dynamics

$$\dot{x}_i \,=\, [A]_{ii}\, x_i \,-\, \frac{1}{2}\sum_{j=1}^{N}(i-j)\,(x_i \,-\, x_j) \,+\, [B_1]_{ii}\, d_i \,+\, [B_2]_{ii}\, u_i,$$

where $[\,\cdot\,]_{ij}$ denotes the ijth block of a matrix and

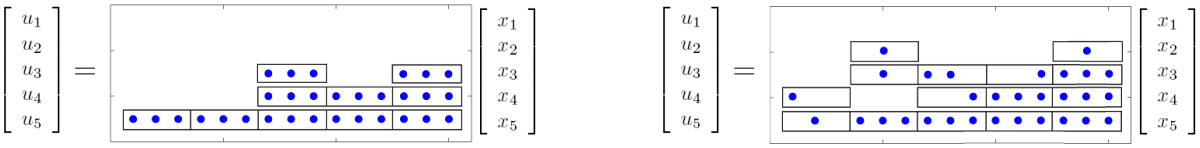
$$[A]_{ii} \,=\, \begin{bmatrix} -1 & 0 & -3 \\ 3 & -1 & 0 \\ 0 & 3 & -1 \end{bmatrix}, \quad [B_1]_{ii} \,=\, \begin{bmatrix} 3 & 0 & 0 \\ 0 & 3 & 0 \\ 0 & 0 & 3 \end{bmatrix}, \quad [B_2]_{ii} \,=\, \begin{bmatrix} 3 \\ 0 \\ 0 \end{bmatrix}.$$

The performance weights Q and R are set to identity matrices. Systems of this form arise in bio-chemical reactions with a cyclic negative feedback [54].

We use the weighted sum of Frobenius norms as the sparsity-promoting penalty function and we set the weights W_{ij} to be inversely proportional to the Frobenius norm of the solution $F^\star_{ij}$ to (SP) at the previous value of γ, i.e., $W_{ij} = 1/(\|F^\star_{ij}\|_F + \varepsilon)$ with $\varepsilon = 10^{-3}$. As γ increases, the number of *nonzero blocks* in the feedback gain F decreases. Figure 11 shows sparsity patterns of feedback gains resulting from solving (SP) with sparse and block sparse penalty functions. Setting γ to values that yield the same number of nonzero elements in these feedback gains results in the block sparse feedback gain with a smaller number of nonzero blocks. In particular, the first two rows of the block sparse feedback gain in Fig. 11a are identically equal to zero (indicated by blank space). This means that the subsystems 1 and 2 do not need to be actuated. Thus, the communication graph determined by the block sparse feedback gain has fewer links; cf. Figs. 12a and 12b.

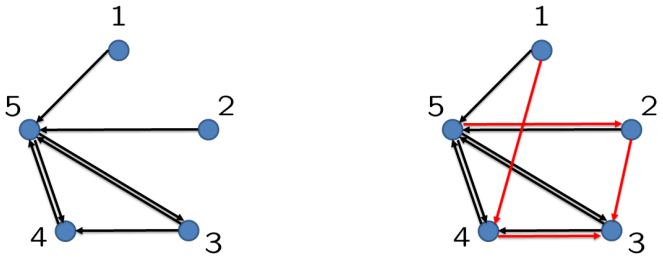
VI. Concluding Remarks

We design sparse and block sparse state feedback gains that optimize the $\mathcal{H}_2$ performance of distributed systems. The design procedure consists of a structure identification step and a polishing step. In the identification step, we employ the ADMM algorithm to solve the sparsity-promoting optimal control problem, whose solution gradually moves from the centralized gain to the sparse gain of interest as our emphasis on the sparsity-promoting penalty term is increased. In the polishing step, we use Newton's method in conjunction with conjugate gradient scheme to solve the minimum variance problem subject to the identified sparsity constraints. We



(a) (b)

Fig. 11: The sparse feedback gains obtained by solving (SP) (a) using the weighted sum of Frobenius norms with $\gamma = 3.6$ and (b) using the weighted ℓ_1 norm (10) with $\gamma = 1.3$. Here, $F \in \mathbb{R}^{5\times 15}$ is partitioned into 25 blocks $F_{ij} \in \mathbb{R}^{1\times 3}$. Both feedback gains have the same number of nonzero elements (indicated by dots) and close $\mathcal{H}_2$ performance (less than 1% difference), but different number of nonzero blocks (indicated by boxes).



(a) (b)

Fig. 12: Communication graphs of (a) the block sparse feedback gain in Fig. 11a and (b) the sparse feedback gain in Fig. 11b (red color highlights the additional links). An arrow pointing from node i to node j indicates that node i uses state measurement from node j.

also establish convexity for a class of feedback synthesis problems that arise in the design of sparse undirected networks. This is accomplished by providing an SDP formulation for design problems ranging from average consensus, to cooperative control of vehicular formations, to synchronization of oscillator networks.

Although we focus on the $\mathcal{H}_2$ performance, the developed framework can be extended to design problems with other performance indices. We emphasize that the analytical solutions to the G-minimization problem are independent of the assigned performance index. Consequently, the G-minimization step in ADMM for (SP) with alternative performance indices can be done exactly as in Section IV-A. Thus, ADMM provides a flexible framework for sparsity-promoting optimal control problems of the form (SP).

We have recently employed ADMM for selection of an *a priori* specified number of leaders in order to minimize the variance of stochastically forced dynamic networks [42], for adding

social links to maximize public awareness in social networks [44], and for identifying sparse representations of consensus networks [55]. We also aim to extend the developed framework to the observer-based sparse optimal feedback design. Another topic of interest is the development of distributed schemes for the F-minimization step in the ADMM algorithm. Recently developed tools from distributed optimization [56] may play an important role in this effort.

ACKNOWLEDGEMENTS

We have benefited tremendously from a lecture series on convex optimization that Stephen P. Boyd taught at UC Santa Barbara as the inaugural Petar Kokotovic Distinguished Visiting Professor. We would like to thank him for inspiring discussions on cardinality minimization problems, ADMM, and group lasso, and to Roland Glowinski for his insightful comments on convergence of ADMM algorithm.

APPENDIX

A. *Proof of Lemma 1*

From the LMI in (16), it follows that $\bar{F} := F + \mathbb{1}\mathbb{1}^T/N \succeq 0$. We next show that $\bar{F}$ is positive definite, $\bar{F} \succ 0$. Using the generalized Schur complement [27, Appendix A.5.5], we have

$$(I - \bar{F}\bar{F}^\dagger)Q^{1/2} \,=\, 0, \tag{28}$$

where $\bar{F}^\dagger$ is the Moore-Penrose pseudoinverse of $\bar{F}$. Consider the spectral decomposition $Q = U\Lambda U^T$ where $U = [\,\frac{1}{\sqrt{N}}\mathbb{1} \;\; V\,]$ is the orthonormal matrix and $\Lambda = \mathrm{diag}\,(\lambda)$ with $\lambda = [\,0 \;\lambda_2 \;\cdots\; \lambda_N\,]$ and $\lambda_i > 0$ for $i = 2, \ldots, N$. Then multiplying U^T from the left and U from the right to (28) yields

$$U^T(I - \bar{F}\bar{F}^\dagger)U\Lambda^{1/2} \,=\, 0.$$

It follows that the symmetric matrix $U^T(I - \bar{F}\bar{F}^\dagger)U$ is a diagonal matrix with its diagonal equal to 0 from the 2nd to the Nth entry, i.e.,

$$U^T(I - \bar{F}\bar{F}^\dagger)U \,=\, \mathrm{diag}\,([\,a \;0 \;\cdots\; 0\,])\,,$$

and thus,

$$\bar{F}\bar{F}^\dagger \,=\, I - (a/N)\mathbb{1}\mathbb{1}^T,$$

where the scalar a is to be determined. We note that $a \neq 1$, because otherwise $\bar{F}\bar{F}^\dagger = I - \mathbb{1}\mathbb{1}^T/N$ implies that the range space of $\bar{F}$ is orthogonal to $\mathbb{1}$ (i.e., $\bar{F}\mathbb{1} = 0$), which leads to the contradiction

$$0 \,=\, \bar{F}\mathbb{1} \,=\, (F + \mathbb{1}\mathbb{1}^T/N)\mathbb{1} \,=\, \mathbb{1}.$$

Since $I-(a/N)\mathbb{1}\mathbb{1}^T$ is not invertible for any $a \neq 1$, we conclude that $\bar{F}$ is of full rank. Therefore, $\bar{F} \succ 0$ and $\bar{F}\bar{F}^\dagger = I$; thus, $a = 0$. Then the equivalence between (15) and (16) can be established by noting that

$$\left[\begin{array}{cc} X & Q^{1/2} \\ Q^{1/2} & \bar{F} \end{array} \right] \succeq 0 \iff X \succeq Q^{1/2}\bar{F}^{-1}Q^{1/2}$$

whenever $\bar{F} \succ 0$. To minimize the objective function of (16) for $\bar{F} \succ 0$, we simply take $X = Q^{1/2}\bar{F}^{-1}Q^{1/2}$, which yields the objective function J in (15). This completes the proof.

B. Formulae for the gradient and Hessian of J in (13) and (14)

We begin by writing the symmetric gain F in (14) using the incidence matrix

$$F \,=\, EK_rE^T \,=\, \sum_{i,j} k_{ij}\, e_{ij}\, e_{ij}^T$$

where K_r is a diagonal matrix with its diagonal determined by $k_r = [\, k_{12} \;\cdots\; k_{(N-1)N} \,] \in \mathbb{R}^m$ with $m = N(N-1)/2$, and E is the incidence matrix of a complete graph [15], [57], defined as $E = [\, e_{12} \;\cdots\; e_{(N-1)N} \,] \in \mathbb{R}^{N\times m}$. Here, $e_{ij} \in \mathbb{R}^N$ takes 1 and -1 at the ith and jth entries, respectively, and 0 otherwise, and i goes from 1 to N and j goes from $i+1$ to N for a fixed i.

The gradient and Hessian of J in (14) with respect to k_r are given by

$$\begin{aligned} \nabla_{k_r} J \,&=\, -\,(1/2)\,\mathrm{diag}\left(E^T(F + \mathbb{1}\mathbb{1}^T/N)^{-1}Q(F + \mathbb{1}\mathbb{1}^T/N)^{-1}E \,-\, E^TRE\right) \\ \nabla^2_{k_r} J \,&=\, (E^T(F + \mathbb{1}\mathbb{1}^T/N)^{-1}Q(F + \mathbb{1}\mathbb{1}^T/N)^{-1}E) \circ (E^T(F + \mathbb{1}\mathbb{1}^T/N)^{-1}E). \end{aligned}$$

The detailed derivation is omitted for brevity; see [57] for related results. For the objective function (13), the symmetric gain F can be written as

$$F \,=\, EK_rE^T \,+\, K_a \,=\, [\, E \;\, I \,] \left[\begin{array}{cc} K_r & O \\ O & K_a \end{array} \right] \left[\begin{array}{c} E^T \\ I \end{array} \right]$$

where K_a is a diagonal matrix with its diagonal determined by $k_a = [\, k_{11} \ \cdots \ k_{NN} \,] \in \mathbb{R}^N$. Let $\bar{E} := [\, E \ I \,] \in \mathbb{R}^{(N+m)\times N}$ and let $\kappa := [\, k_r^T \ k_a^T \,]^T \in \mathbb{R}^{N+m}$. Then the gradient and Hessian of J in (13) with respect to κ are given by

$$\begin{aligned} \nabla_\kappa J \ &= \ -\,(1/2)\,\mathrm{diag}\left(\bar{E}^T F^{-1} Q F^{-1} \bar{E} \ - \ \bar{E}^T R \bar{E}\right) \\ \nabla^2_\kappa J \ &= \ (\bar{E}^T F^{-1} Q F^{-1} \bar{E}) \circ (\bar{E}^T F^{-1} \bar{E}). \end{aligned}$$

C. Derivation of (25)-(26)

The first step is to show that the minimizer of ϕ_{ij} can be written as $G^\star_{ij} = r V_{ij}$ where $r \in [0,1]$. This can be seen by noting that for $V_{ij} > 0$, we have $G^\star_{ij} \in [0, V_{ij}]$ since both the logarithmic function $\log(1 + |G_{ij}|/\varepsilon)$ and the quadratic function $(G_{ij} - V_{ij})^2$ are monotonically increasing for $G_{ij} \geq V_{ij}$ and monotonically decreasing for $G_{ij} \leq 0$. A similar arguments shows that $G^\star_{ij}$ belongs to $[V_{ij}, 0]$ for $V_{ij} < 0$. Thus, minimizing $\phi_{ij}(G_{ij})$ is equivalent to minimizing

$$\phi_{ij}(r) \ = \ \gamma \log\left(1 + \frac{|V_{ij}| r}{\varepsilon}\right) \ + \ \frac{\rho}{2} V_{ij}^2 (r-1)^2$$

subject to the constraint $0 \leq r \leq 1$. Thus, we have converted a nondifferentiable unconstrained problem to a differentiable but constrained one.

We will now examine the sign of $\partial\phi_{ij}/\partial r$ for $r \in [0,1]$. Setting $\partial\phi_{ij}/\partial r = 0$ yields a quadratic equation (for $V_{ij} \neq 0$)

$$|V_{ij}| r^2 \ + \ (\varepsilon - |V_{ij}|) r + \frac{\gamma}{\rho |V_{ij}|} - \varepsilon = 0. \tag{29}$$

If the discriminant $\Delta \leq 0$, then $\partial\phi_{ij}/\partial r \geq 0$ and ϕ_{ij} is monotonically nondecreasing for $r \in [0,1]$; thus, the minimizer is $r^\star = 0$. Let us assume that $\Delta > 0$ and let $r^\pm$ be the solutions to (29). It is then readily verified that

$$r^\pm \ = \ \frac{1}{2|V_{ij}|}\left(|V_{ij}| - \varepsilon \pm \sqrt{(|V_{ij}| + \varepsilon)^2 - 4(\gamma/\rho)}\right) \ \leq \ 1.$$

Then the sign of $\partial\phi_{ij}/\partial r$ for $r \in [0,1]$ can be determined by checking the values of $r^\pm$.

1) If $r^\pm \leq 0$, then $\partial\phi_{ij}/\partial r > 0$ for $r \in [0,1]$; thus, the minimizer is $r^\star = 0$.
2) If $r^- \leq 0$ and $0 < r^+ \leq 1$, then $\partial\phi_{ij}/\partial r \leq 0$ for $r \in [0, r^+]$ and $\partial\phi_{ij}/\partial r > 0$ for $r \in (r^+, 1]$; thus, the minimizer is $r^\star = r^+$.

3) Finally, if $0 \leq r^{\pm} \leq 1$, then $\partial\phi_{ij}/\partial r \geq 0$ for $r \in [0, r^-)$, $\partial\phi_{ij}/\partial r \leq 0$ for $r \in [r^-, r^+)$, and $\partial\phi_{ij}/\partial r \geq 0$ for $r \in [r^-, 1]$. Therefore, r^- is a local maximizer and r^+ is a local minimizer. Thus, the candidates for $r^\star$ are $\{0, r^+\}$.

REFERENCES

[1] B. Bamieh, F. Paganini, and M. A. Dahleh, "Distributed control of spatially invariant systems," *IEEE Trans. Automat. Control*, vol. 47, no. 7, pp. 1091–1107, 2002.

[2] G. A. de Castro and F. Paganini, "Convex synthesis of localized controllers for spatially invariant system," *Automatica*, vol. 38, pp. 445–456, 2002.

[3] P. G. Voulgaris, G. Bianchini, and B. Bamieh, "Optimal H^2 controllers for spatially invariant systems with delayed communication requirements," *Syst. Control Lett.*, vol. 50, pp. 347–361, 2003.

[4] R. D'Andrea and G. E. Dullerud, "Distributed control design for spatially interconnected systems," *IEEE Trans. Automat. Control*, vol. 48, no. 9, pp. 1478–1495, 2003.

[5] C. Langbort, R. S. Chandra, and R. D'Andrea, "Distributed control design for systems interconnected over an arbitrary graph," *IEEE Trans. Automat. Control*, vol. 49, no. 9, pp. 1502–1519, 2004.

[6] B. Bamieh and P. G. Voulgaris, "A convex characterization of distributed control problems in spatially invariant systems with communication constraints," *Syst. Control Lett.*, vol. 54, pp. 575–583, 2005.

[7] M. Rotkowitz and S. Lall, "A characterization of convex problems in decentralized control," *IEEE Trans. Automat. Control*, vol. 51, no. 2, pp. 274–286, 2006.

[8] N. Motee and A. Jadbabaie, "Optimal control of spatially distributed systems," *IEEE Trans. Automat. Control*, vol. 53, no. 7, pp. 1616–1629, 2008.

[9] F. Borrelli and T. Keviczky, "Distributed LQR design for identical dynamically decoupled systems," *IEEE Trans. on Automat. Control*, vol. 53, no. 8, pp. 1901–1912, 2008.

[10] M. Fardad, F. Lin, and M. R. Jovanović, "On the optimal design of structured feedback gains for interconnected systems," in *Proceedings of the 48th IEEE Conference on Decision and Control*, 2009, pp. 978–983.

[11] P. Shah and P. A. Parrilo, "H_2 optimal decentralized control over posets: A state space solution for state-feedback," in *Proceedings of the 49th IEEE Conference on Decision and Control*, 2010, pp. 6722–6727.

[12] J. Swigart and S. Lall, "An explicit state-space solution for a decentralized two-player optimal linear-quadratic regulator," in *Proceedings of the 2010 American Control Conference*, 2010, pp. 6385–6390.

[13] M. R. Jovanović, "On the optimality of localized distributed controllers," *Int. J. Systems, Control and Communications*, vol. 2, no. 1/2/3, pp. 82–99, 2010.

[14] M. Fardad and M. R. Jovanović, "Design of optimal controllers for spatially invariant systems with finite communication speed," *Automatica*, vol. 47, no. 5, pp. 880–889, 2011.

[15] D. Zelazo and M. Mesbahi, "Edge agreement: Graph-theoretic performance bounds and passivity analysis," *IEEE Trans. Automat. Control*, vol. 56, no. 3, pp. 544–555, 2011.

[16] F. Lin, M. Fardad, and M. R. Jovanović, "Augmented Lagrangian approach to design of structured optimal state feedback gains," *IEEE Trans. Automat. Control*, 2011, doi:10.1109/TAC.2011.2160022.

[17] L. Lessard and S. Lall, "Optimal controller synthesis for the decentralized two-player problem with output feedback," in *Proceedings of the 2012 American Control Conference*, 2012, pp. 6314–6321.

[18] F. Lin, M. Fardad, and M. R. Jovanović, "Optimal control of vehicular formations with nearest neighbor interactions," *IEEE Trans. Automat. Control*, 2012, doi:10.1109/TAC.2011.2181790; also arXiv:1112.4113v1.

[19] S. Boyd, N. Parikh, E. Chu, B. Peleato, and J. Eckstein, "Distributed optimization and statistical learning via the alternating direction method of multipliers," *Foundations and Trends in Machine Learning*, vol. 3, no. 1, pp. 1–124, 2011.

[20] E. J. Candès and T. Tao, "Near optimal signal recovery from random projections: Universal encoding strategies?" *IEEE Trans. Inf. Theory*, vol. 52, no. 12, pp. 5406–5425, 2006.

[21] T. Hastie, R. Tibshirani, and J. Friedman, *The elements of statistical learning*. Springer, 2009.

[22] E. J. Candès, M. B. Wakin, and S. P. Boyd, "Enhancing sparsity by reweighted ℓ_1 minimization," *Journal of Fourier Analysis and Applications*, vol. 14, pp. 877–905, 2008.

[23] S. Schuler, C. Ebenbauer, and F. Allgöwer, "ℓ_0-system gain and ℓ_1-optimal control," in *Preprints of the 18th IFAC World Congress*, 2011, pp. 9230–9235.

[24] S. Schuler, P. Li, J. Lam, and F. Allgöwer, "Design of structured dynamic output-feedback controllers for interconnected systems," *International Journal of Control*, 2011, doi:10.1080/00207179.2011.634029.

[25] S. Schuler, M. Gruhler, U. Münz, and F. Allgöwer, "Design of structured static output feedback controllers," in *Preprints of the 18th IFAC World Congress*, 2011, pp. 271–276.

[26] D. Zelazo, S. Schuler, and F. Allgöwer, "Performance and design of cycles in consensus networks," *Syst. Control Lett.*, 2012, submitted.

[27] S. Boyd and L. Vandenberghe, *Convex Optimization*. Cambridge University Press, 2004.

[28] M. S. Lobo, M. Fazel, and S. Boyd, "Portfolio optimization with linear and fixed transaction costs," *Ann. Oper. Res.*, vol. 152, pp. 341–365, 2007.

[29] M. Fardad, F. Lin, and M. R. Jovanović, "Sparsity-promoting optimal control for a class of distributed systems," in *Proceedings of the 2011 American Control Conference*, 2011, pp. 2050–2055.

[30] M. Fardad, F. Lin, and M. R. Jovanović, "On the optimal synchronization of oscillator networks via sparse interconnection graphs," in *Proceedings of the 2012 American Control Conference*, Montréal, Canada, 2012, pp. 4777–4782.

[31] P. L. D. Peres and J. C. Geromel, "An alternate numerical solution to the linear quadratic problem," *IEEE Trans. Automat. Control*, vol. 39, pp. 198–202, 1994.

[32] R. Olfati-Saber and R. M. Murray, "Consensus problems in networks of agents with switching topology and time-delays," *IEEE Trans. Automat. Control*, vol. 49, no. 9, pp. 1520–1533, 2004.

[33] L. Xiao, S. Boyd, and S.-J. Kim, "Distributed average consensus with least-mean-square deviation," *Journal of Parallel and Distributed Computing*, vol. 67, no. 1, pp. 33–46, 2007.

[34] G. F. Young, L. Scardovi, and N. E. Leonard, "Robustness of noisy consensus dynamics with directed communication," in *Proceedings of the 2010 American Control Conference*, 2010, pp. 6312–6317.

[35] M. Mesbahi and M. Egerstedt, *Graph Theoretic Methods in Multiagent Networks*. Princeton University Press, 2010.

[36] B. Bamieh, M. R. Jovanović, P. Mitra, and S. Patterson, "Coherence in large-scale networks: dimension dependent limitations of local feedback," *IEEE Trans. Automat. Control*, 2012, in press; also arXiv:1112.4011v1.

[37] F. Lin, M. Fardad, and M. R. Jovanović, "On the optimal localized feedback design for multi-vehicle systems," in *Proceedings of the 49th IEEE Conference on Decision and Control*, 2010, pp. 5744–5749.

[38] S. Patterson and B. Bamieh, "Network coherence in fractal graphs," in *Proceedings of the 50th IEEE Conference on Decision and Control and European Control Conference*, 2011, pp. 6445–6450.

[39] F. Lin, M. Fardad, and M. R. Jovanović, "Performance of leader-follower consensus algorithms in directed trees and lattices," in *Proceedings of the 51st IEEE Conference on Decision and Control*, 2012, to appear.

[40] A. Ghosh and S. Boyd, "Growing well-connected graphs," in *Proceedings of the 45th IEEE Conference on Decision and Control*, 2006, pp. 6605–6611.

[41] S. Patterson and B. Bamieh, "Leader selection for optimal network coherence," in *Proceedings of the 49th IEEE Conference on Decision and Control*, 2010, pp. 2692–2697.

[42] F. Lin, M. Fardad, and M. R. Jovanović, "Algorithms for leader selection in large dynamical networks: noise-corrupted leaders," in *Proceedings of the 50th IEEE Conference on Decision and Control and European Control Conference*, 2011, pp. 2932–2937.

[43] M. Fardad, F. Lin, and M. R. Jovanović, "Algorithms for leader selection in large dynamical networks: noise-free leaders," in *Proceedings of the 50th IEEE Conference on Decision and Control and European Control Conference*, 2011, pp. 7188–7193.

[44] M. Fardad, X. Zhang, F. Lin, and M. R. Jovanović, "On the optimal dissemination of information in social networks," in *Proceedings of the 51st IEEE Conference on Decision and Control*, 2012, to appear.

[45] H. Zhu, G. B. Giannakis, and A. Cano, "Distributed in-network channel decoding," *IEEE Trans. Signal Process.*, vol. 57, no. 10, pp. 3970–3983, 2009.

[46] T. Goldstein and S. Osher, "The split Bregman method for ℓ_1 regularized problems," *SIAM Journal on Imaging Sciences*, vol. 2, no. 2, pp. 323–343, 2009.

[47] P. A. Forero, A. Cano, and G. B. Giannakis, "Consensus-based distributed support vector machines," *Journal of Machine Learning Research*, vol. 11, pp. 1663–1707, 2010.

[48] P. M. Mäkilä and H. T. Toivonen, "Computational methods for parametric LQ problems – a survey," *IEEE Trans. Automat. Control*, vol. 32, no. 8, pp. 658–671, 1987.

[49] T. Rautert and E. W. Sachs, "Computational design of optimal output feedback controllers," *SIAM J. Optim.*, vol. 7, no. 3, pp. 837–852, 1997.

[50] J. Nocedal and S. J. Wright, *Numerical Optimization*. Springer, 2006.

[51] M. Fortin and R. Glowinski, *Augmented Lagrangian method: Application to the numerical solution of boundary-value problems*. North-Holland, 1983.

[52] R. Glowinski and P. Le Tallec, *Augmented Lagrangian and operator-splitting methods in nonlinear mechanics*. SIAM, 1989.

[53] D. G. Luenberger and Y. Ye, *Linear and Nonlinear Programming*. Springer, 2008.

[54] M. R. Jovanović, M. Arcak, and E. D. Sontag, "A passivity-based approach to stability of spatially distributed systems with a cyclic interconnection structure," *IEEE Trans. Automat. Control: Special Issue on Systems Biology*, vol. 53, pp. 75–86, 2008.

[55] N. Dhingra, F. Lin, M. Fardad, and M. R. Jovanović, "On identifying sparse representations of consensus networks," in *Proceedings of the 3rd IFAC Workshop on Distributed Estimation and Control in Networked Systems*, 2012, to appear.

[56] A. Nedić and A. Ozdaglar, "Cooperative distributed multi-agent optimization," in *Convex Optimization in Signal Processing and Communications*. Cambridge University Press, 2010.

[57] A. Ghosh, S. Boyd, and A. Saberi, "Minimizing effective resistance of a graph," *SIAM Review*, vol. 50, no. 1, pp. 37–66, 2008.